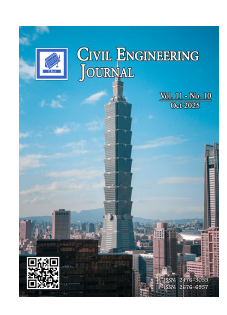


Civil Engineering Journal

(E-ISSN: 2476-3055; ISSN: 2676-6957)

Vol. 11, No. 10, October, 2025



Data-Driven Approach to Predict Fire-Resistance Ratings of Timber Columns

Tu T. Nguyen ¹, Hung T. Pham ²*₀, Hung K. Nguyen ¹

¹ Faculty of Civil Engineering, Lac Hong University, Dong Nai Province, Viet Nam.

Received 01 March 2025; Revised 21 September 2025; Accepted 28 September 2025; Published 01 October 2025

Abstract

This study aims to determine whether a data-driven-based approach provides more accurate predictions of timber fire-resistance ratings (FRR) compared to conventional empirical methods. To achieve this, a machine learning framework based on the Deep Belief Network (DBN) was employed. A comprehensive database collected from previously published reports was used to train and validate the DBN model. The model's predictive performance was benchmarked against traditional empirical equations derived from mechanics-based methods. The comparison demonstrated that the DBN model provided superior accuracy in predicting fire-resistance ratings. Model evaluation was further conducted using the Coefficient of Determination (R^2) and Root Mean Squared Error (RMSE), confirming the robustness of the proposed approach. In addition, a parametric analysis was performed to assess the influence of input variables on the output. Results indicated that induced load (IDL) and breadth (BRH) were the most influential parameters, whereas ultimate strength (ULS) and elasticity modulus (ELM) had relatively minor effects. This study highlights the potential of advanced machine learning techniques, particularly DBN, to enhance predictive accuracy in structural fire engineering, offering a significant improvement over conventional calculation methods.

Keywords: Fire-Resistance Rating; Timber Column; Wood Structures; Machine Learning; Deep Belief Network; Parameter Analysis.

1. Introduction

Structures using green and sustainable materials have gained much recognition over the past decade. Thanks to its incredible properties, such as pleasing appearance, ease of use, and necessary fire resistance, timber has been widely used for exposed structural members of modern structures [1]. The applications of advanced engineered timber products for constructing mid-rise and tall wood buildings are becoming more and more popular worldwide [2]. As an example, a 122,000 square-foot (11300 square-meter) building that used glulam and laminated timber beams was constructed in Norway in 2019, with a height of approximately 90 meters and 18 stories, making it the highest timber structure in the world [3]. Japan has also proposed an ambitious concept design to build a 70-story wood-framed tower in Tokyo, called *W350*. Timber and steel would be utilized in this building, with wooden materials accounting for 90 percent [4].

To make engineered timber products possible for high-rise buildings, intensive investigations have been conducted to study structural performances and building management [5-10], as well as the fire response behavior of advanced and sustainable materials [1, 11-19]. Girompaire & Dagenais [11] developed an analytical model to predict fire dynamics in mass timber compartments with exposed surfaces. The model's predictions of temperature, char depth, and heat release rate were compared against 20 experimental compartment fires, both with and without exposed timber. The results of

^{*} Corresponding author: hungpt@hau.edu.vn





© 2025 by the authors. Licensee C.E.J, Tehran, Iran. This article is an open access article distributed under the terms and conditions of the Creative Commons Attribution (CC-BY) license (http://creativecommons.org/licenses/by/4.0/).

² Faculty of Civil Engineering, Hanoi Architectural University, Hanoi, Viet Nam.

this study showed strong agreement between the model predictions and the experimental data. Wiesner et al. [12] performed a series of large-scale experiments on cross-laminated timber (CLT) slabs subjected to four different heating scenarios with varying profiles to validate a previously published structural model. The findings confirmed that the proposed structural fire model can accurately predict the timber's load-bearing capacity during fire. For assessing fire performance, ASTM E119 Standard Test Methods for Fire Tests of Building Construction and Materials [20] provides the procedures for determining the FRR of structural timber members, while the minimum fire-resistance requirements for building systems are specified in the 2015 International Building Code [21]. Besides, the *National Design Specification for Wood Construction* (NDS) [22] also outlined the fire design concepts for timber assemblies (i.e., beam, column, floor).

The fire exposure time of a column depends on different factors such as the induced load, the ratio between induced load and ultimate capacity, the char rate, the loss of initial breadth, B, and depth, D, and the slenderness ratio (L_e/D) of a member (L_e is the effective length of the corresponding column). Figure 1 illustrates the cross-section of a rectangular column with fire exposed on four sides. The loss of cross-section at the corners of the column is faster than that of other parts due to the corner being heated from two sides. The high char rate develops the rounding effect at these corners, making the remaining cross-section of the column no longer rectangular after fire [1].

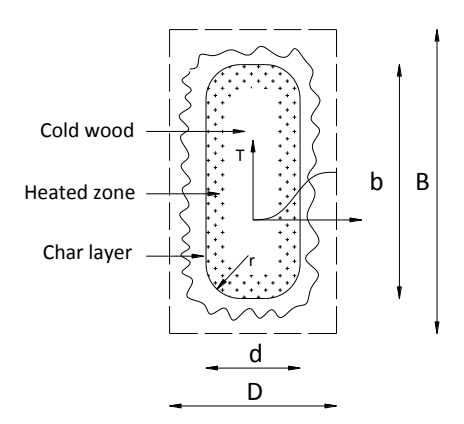


Figure 1. Reduction in dimensions due to charging

The fire exposure time is determined at the point where the column fails due to the stress in the remaining section being over the maximum stress capacity. Depending on the column slenderness ratio, the column failure either occurs when the maximum compressive capacity surpasses its limit for the case of short column members or due to exceeding critical buckling capacity for the long column members. The NDS [22] provided equations to calculate a stability factor that is used for estimating the column capacity. The critical section of the column is determined through an iterative calculation using Equation 1 for the short column and Equation 2 for the long column.

$$k Z B D = \alpha b d \tag{1}$$

$$k Z \frac{B D^3}{12} = \alpha \frac{b d^3}{12} \tag{2}$$

where k is the safety factor reduction; Z is the load factor; b and d are the remaining breadth and depth of the section after a fire, respectively; α is the uniform reduction in strength properties; D is the column's smallest cross-sectional dimension, with buckling assumed in this weakest direction.

In the past, the FRR of the timber columns was estimated by employing the method developed by Lie [23]. In this method, the reduction of the member section was calculated using a constant char rate of β = 1.42 in/hour (3.6 cm/hour), the rounding effects at the corners due to the increasing char rate were omitted. Also, a factor k = 0.33, and $\alpha = 0.8$ accounts for the design-to-ultimate strength ratio and strength and stiffness reductions. For the four-sided exposure, Equation 3 (in the US unit) was applied to estimate FRR.

$$t_f = 2.54 \ Z \ D\left(3 - \frac{D}{R}\right) \tag{3}$$

where Z for short column $(L_e/D \le 11)$ can be calculated from:

$$Z = \begin{cases} 1.5 & R < 0.5 \\ 0.9 + \frac{0.3}{R} & R \ge 0.5 \end{cases} \tag{4}$$

For the long column ($L_e/D > 11$), Z can be computed by Equation 5:

$$Z = \begin{cases} 1.3 & R < 0.5 \\ 0.7 + \frac{0.3}{R} & R \ge 0.5 \end{cases}$$
 (5)

where R is applied to the allowable load ratio.

In current practice, the adaptive mechanics-based design method is utilized to calculate the FRR of column members. Instead of using a fixed char rate, β , as in the Lie method, an adaptive effective char rate, β_{eff} , is used. The effective char rate is a nonlinear function of time exposure t, and nominal char rate value β_n , and is determined by Equation 6. In this Equation, a coefficient of 1.2 accounts for corner rounding and strength and stiffness reductions in the heated zone.

$$\beta_{eff} = \frac{1.2 \, \beta_n}{t^{0.187}} \tag{6}$$

The section properties of the columns subjected to four-sided exposure can be calculated using equations presented in Table 1 (Table 16.2.1 in NDS [22]). Gagnon & Pirvu (Wood Handbook) [24] stated that an FRR is the period during which a building element, component, or assembly can maintain its separating function, preventing or slowing the spread of heat, flames, or hot gases, its load-bearing function, or both." To determine the FRR of a timber member, the standard fire-resistance tests compliant with ASTM E119-20 [20] are performed. The tested members are evaluated via three acceptance criteria, namely (i) structural resistance, (ii) integrity, and (iii) insulation. The standard time-temperature relationship used in fire-resistance testing is shown in Figure 2.

Table 1. Cross-sectional properties for four-sided exposure (in US unit)

Cross-sectional property	Equations
Area of the cross-section, in ²	$A(t) = (B - 2b_{eff}t) (D - 2b_{eff}t)$
Section Modulus about the major axis, in ³	$S(t) = (B - 2b_{eff}t) (D - 2b_{eff}t)^2/6$
Section Modulus about the minor axis, in ³	$S(t) = (B - 2b_{eff}t)^2(D - 2b_{eff}t)/6$
Moment of Inertia about the major axis, in ⁴	$I(t) = (D_{min} - 2b_{eff}t) (D_{max} - 2b_{eff}t)^3/12$
Moment of Inertia about the minor axis, in ⁴	$I(t) = (D_{min} - 2b_{eff}t)^3 (D_{max} - 2b_{eff}t)/12$

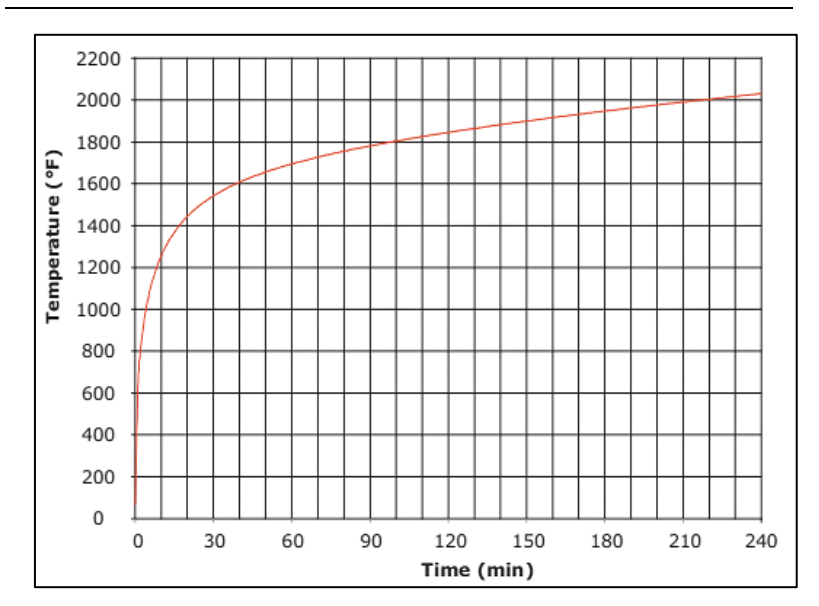


Figure 2. Standard time-temperature relationship [20]

Regarding the approval conditions, Figure 3 illustrates three acceptance criteria for timber members/assemblies. The first benchmark is the structural resistance, which is related to the stability of the tested members/assemblies under structural load during the fire test. The second benchmark, integrity standards, is linked to the passing of flame or hot gases through tested structures. The last measure is related to the maximum acceptable surface temperature of the tested members/assemblies. Information on these acceptance criteria can be found in detail in the Wood Handbook [24]. The FRR indicates the time at which a component fails to comply with at least one of the three criteria.

Figure 3. Structural fire performance requirements [24]

The conventional methods to estimate FRR for timber structures either utilize standard fire tests or apply empirical equations. Recently, the technique employing machine learning-based (ML) models, such as DBN or ANN, can be applied for timber FRR estimation. Instead of relying on purely mathematical equations, machine learning-based models use adaptive learning techniques to capture the nonlinear hidden relationship between inputs and outputs through existing experimental data. After training and testing with available data, the successfully developed models can be used to predict the outputs from the new input dataset with a high rate of accuracy.

Regarding the applications of the ML-based models in assessing the fire performance of timber, Tasdemir et al. [25] employed ML to estimate the final cross-section of the timber after a fire with 180 experimental records. Evidence suggests that the ML model effectively predicted the remaining section of timber after the fire. Cachim [26] employed a multilayer feed-forward network model to estimate the temperature in the timber under fire loading using numerical data. The ML model was also successfully applied to predict the thermal and structural properties of timbers at the material and elemental level in a study by Naser [27]. Zaker Esteghamati et al. [28] developed interpretable machine learning models to predict the fire resistance of timber columns using 70 experimental records, taking into account their geometry and material properties. The study demonstrated that Random Forest (RF) models outperformed traditional prescriptive approaches, providing greater prediction accuracy while improving the interpretability of the results.

In a recent study, Lou et al. [29] employed a DeepONet-based approach combined with finite element (FE) data to develop an integrated computational framework for analyzing and predicting temperature fields in glulam beam—column connections exposed to fire. The study demonstrated outstanding predictive performance, achieving an R² of 0.9991, while operating substantially faster than conventional FE analyses. Ye et al. [30] employed an FE-based ML model to predict the real-time structural response of a steel frame from temperature data under hundreds of fire scenarios. Several ML models were developed and trained with temperature as input and displacement as output. The results showed that Gradient Boosting achieved the highest accuracy, with an R² value of 0.99 when trained on 1,000 fire scenarios. ML was also used in the study of Ishtiaq et al. [31] to improve the fire safety of timber structures.

Amin et al. [32] created a data-driven model to estimate the average charring rate of timber in fire, drawing on a database of 231 test samples. The findings showed that the model performed well, achieving predictions with as little as 9% error. The authors further emphasized that the predicted average charring rate provided a much higher level of accuracy compared to the values specified in Eurocode-5, the standard widely used in many countries, and that this improvement was consistent across a wide range of mass timber products. Han et al. [33] developed an explainable machine learning model using numerical data to predict the FRR of connections. The model was validated against 140 experimental data points and demonstrated superior performance compared to conventional empirical equations. Sensitivity analysis further revealed that timber thickness and load ratio are the most influential factors affecting the FRR.

Besides the application for fire-related analysis, machine learning-based models have also been employed to address various engineering problems [34-42]. For example, Fud [34] used the DBN model to forecast the cooling load of the air-conditioning system. The proposed model was validated with real cooling load data from two different locations. It was shown that the DBN model could catch the nonlinear and dynamic features of the cooling load data series with high accuracy. In a study by Rafiei et al. [35], the DBN model was developed using 103 experimental records to predict the compressive strength of concrete at 28 days. The performance accuracy of the proposed DBN model was reported to reach 98 percent.

Hao et al. [36] applied the DBN model with a sliding window to predict multiple-index energy consumption for a cement production plant. A sliding window technique was introduced to eliminate the time-varying delay and improve the performance of the DBN model. In another study, Nguyen et al. [37] employed a DBN model with 288 experimental data records to examine factors affecting ground-penetrating radar signal amplitude in reinforced concrete structures. The model demonstrated excellent predictive performance, achieving an R² of 0.9681 for the entire dataset. Nguyen & Dinh [38] applied ML to estimate bridge deck ratings using data from the National Bridge Inventory, achieving prediction accuracy of up to 98.5%. The ML-based models were employed to detect structural damages [39], to predict cardiovascular diseases [40], or to estimate the hardened properties of concrete [41, 42].

Despite significant progress, the use of DBNs in timber structures, particularly under fire conditions, remains limited. Accurate prediction of the FRR of timber columns is essential for structural fire safety design. Yet, the high cost and labor-intensive nature of fire testing restricts dataset availability and slows the development of reliable predictive models in engineering practice. To address these challenges, this study proposes a DBN model for predicting the FRR of timber columns. Leveraging the strong predictive capabilities of DBNs, the approach provides an efficient and reliable tool for enhancing the fire safety design of timber structures.

In this paper, a DBN approach was employed to predict the FRR of timber columns using data from a previously published study [1]. Proposed DBN model performance was evaluated using various coefficient measures, and its predictions were compared with calculated values reported in earlier publications. Currently, the FRR of timber members is primarily determined through standard fire tests and conventional empirical equations [24]. As far as the authors are aware, no prior studies have applied the DBN method for predicting the FRR of timber columns. The main objective of this research is to assess whether a machine learning—based approach can outperform conventional empirical methods in predicting timber FRR, while also advancing the understanding of how deep learning captures the nonlinear relationships between fire-resistance and its influencing variables. The DBN subroutine was implemented in MATLAB R2022a, following the approach of Tanaka [43].

The subsequent sections are organized as follows. Section 2 describes the data and methodology, including data collection and preprocessing, a brief overview of the DBN model, and the proposed DBN architecture for predicting the FRR of timber structures. Section 3 presents the key results, covering assessment categories, comparison with previously published calculations, and sensitivity analysis. Section 4 offers an in-depth discussion, followed by Section 5, which concludes the paper and suggests directions for future work.

2. Data and Methodology

Experimental data on FRR for timber columns extracted from the previously published source were employed in this study. The original data were refined to obtain a reliable dataset for developing and testing the proposed DBN model. A brief statistical analysis of the input and output variables was also presented. Besides, a summary of the DBN model, the model architecture, and steps to establish the DBN model for estimating the timber FRR were briefly discussed. Detailed information is described in the subsequent sections.

2.1. Data Collection and Pre-Processing

The original dataset consisted of 62 records of timber FRR collected from experimental fire tests. Table 2 presents the input and output variables and their basic statistical value in the entire dataset. It should be pointed out that the dataset also included the FRR calculated from the empirical equations proposed by the Lie method and the adaptive mechanics-based method. The calculated data were later used to compare with the predictions of the proposed DBN model.

Parameter	Symbol	Type	Unit	Min.	Max.
Depth	DEP	Input	in.	5.5	11
Breadth	BRH	Input	in.	5.5	15.75
Specific gravity	SPG	Input	-	0.31	0.59
Ultimate strength	ULS	Input	psi	2565	9003
Elasticity modulus	ELM	Input	$10^6 \mathrm{psi}$	1.0	2.7
Resisting capacity	RCP	Input	lbs	70830	585190
Induced load	IDL	Input	lbs	9520	143960
Measured time from tests	MST	Output	minute	21	76
Rating with the Lie method	-	Other	minute	28	69
Rating mechanics-based method	-	Other	minute	18	96

Table 1. Input and output characteristics

Before using the data for training and testing the proposed DBN model, all dataset values were carefully normalized to fall within the range of [0, 1] to ensure uniform scaling, improve numerical stability, and facilitate more efficient and accurate model learning using Equation 7

$$X_{norm} = \frac{X - X_{min}}{X_{max} - X_{min}} \tag{7}$$

where X and X_{norm} denote the original and normalized values, respectively, while X_{max} and X_{min} represent the maximum and minimum values of X.

2.2. Approach Using Deep Belief Network

A DBN is an unsupervised learning algorithm that uses probabilistic methods to generate outputs. Its typical structure comprises multiple interconnected Restricted Boltzmann Machine (RBM) units, as shown in Figure 4-a, with the first RBM serving as the visible layer and the subsequent units forming the hidden layers.

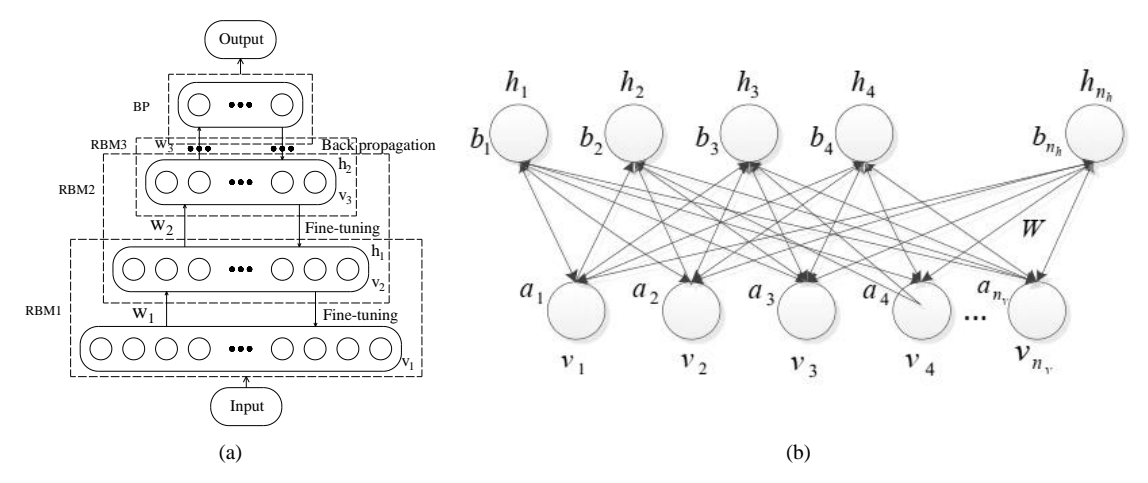


Figure 4. (a) Deep Belief Network structure; (b) Restricted Boltzmann Machine Architecture

A Restricted Boltzmann Machine (RBM) is composed of two layers: a visible layer and a hidden layer. Each neuron in the visible layer is fully connected to every neuron in the hidden layer, but there are no connections among neurons within the same layer [44]. Figure 4-b illustrates a standard RBM architecture, where v_i represents a unit in the visible layer v, and h_i denotes the unit in the hidden layer h. The weight matrix W defines the connections between the two layers. Each visible unit has an associated bias $a_{i,}$ and each hidden unit has a bias b_i . Given a set of states (v, h), the energy of the RBM network can be defined as:

$$E(v,h) = -\sum_{i} a_{i} v_{i} - \sum_{j} b_{j} h_{j} - \sum_{i} \sum_{j} v_{j} w_{i,j} h_{j} = -a^{T} v - b^{T} h - h^{T} w v$$
(8)

The joint probability of an input v with the hidden vector h is described as

$$P(v,h;\theta) = \frac{1}{7}e^{-E(v,h)}$$
 (9)

where $\theta = \{a, b, w\}$ is the RMB network parameter; Z is a normalizing constant event so that the sum of all events equals 1. The marginal distribution of training data v can be obtained by summing over h as:

$$(v) = \frac{1}{z} \sum_{h} e^{-E(v,h)} \tag{10}$$

In the same manner, the marginal probability distribution of the hidden layer can be determined.

$$P(h) = \frac{1}{Z} \sum_{v} e^{-E(v,h)} \tag{11}$$

To train the RBM network, the model parameters in Equation 9 are solved by the maximum likelihood method.

$$ln P(h) = ln \left(\sum_{h} e^{-E(v,h)} \right) - ln \left(\sum_{v} \sum_{h} e^{-E(v,h)} \right)$$
(12)

$$\frac{\partial \ln P(h)}{\partial a} = E_{Pd}[v] - E_{Pm}[v] \tag{13}$$

$$\frac{\partial \ln P(v)}{\partial b} = E_{Pd}[h] - E_{Pm}[h] \tag{14}$$

$$\frac{\partial \ln P(v)}{\partial w} = E_{Pd}[vh^T] - E_{Pm}[vh^T] \tag{15}$$

where E_{Pd} , E_{Pm} denote the expectations of the data and model probability distributions, respectively, computed using the contrastive divergence algorithm [45].

$$P(v_i = 1|h) = \sigma(a_i + \sum_{i=1}^{n} w_{i,i}h_i)$$
(16)

$$(h_i = 1|v) = \sigma(b_i + \sum_{i=1}^m w_{i,i} v_i)$$
(17)

$$\sigma(x) = \frac{1}{1+e^{-x}} \tag{18}$$

DBN is a combination of several RBMs; thus, the joint probability distribution of DBN can be determined by Equation 19

$$P(v, h_1, h_2, ..., h_n) = P(v \mid h_1) P(h_1 \mid h_2), ..., P(h_{n-2} \mid h_{n-1}) P(h_{n-1} \mid h_n)$$
(19)

where $P(h_n | h_{n+1})$ is the conditional probability of h_n for the given h_{n+1} state; $P(h_{n-1} | h_n)$ is the joint probability of h_{n-1} and h_n . P(v, h) represents the joint probability distribution of a single RBM.

2.3. Development of the DBN Model for FRR of Timber Structures

The DBN model has been employed for dealing with unsupervised issues and has proven as an effective solution for energy consumption prediction in the cement calcination process [36], predicting ground penetrating radar signal [37], bearing performance degradation [46], and controlling systems of collaborative robots [47, 48]. In this study, DBN was used to address the supervised problems for estimating the FRR for timber structures using a comprehensive database consisting of 62 experimental fire-testing records of the timber. Table 3 shows the configurations of the proposed DBN model. The methodology used in this study is illustrated in Figure 5.

Table 2. Detailed DBN model configurations

Argument	Quantity	
Input neurons 7		
Output neurons	1	
Number of neurons in hidden layers	15	
Epochs number	50	
Maximum iteration number	100	
Momentum for iterations	0.9	
Learning step size	0.01	
Costs of weight update	0.0002	
Dropout rate	0.2	

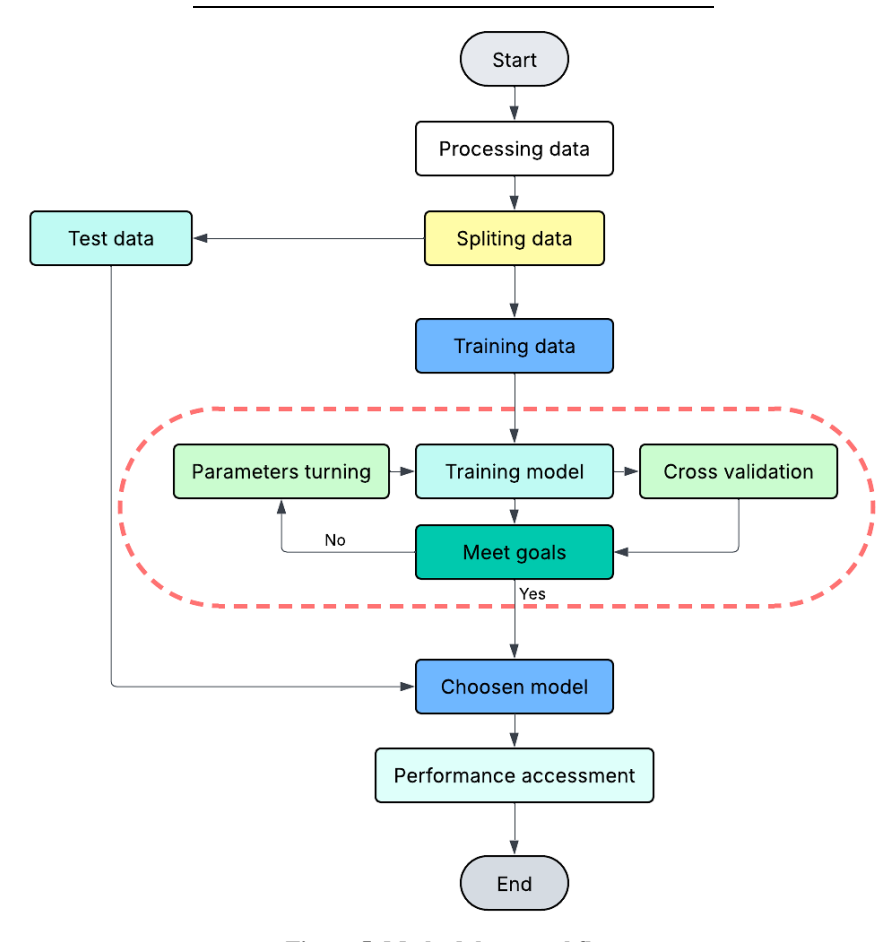


Figure 5. Methodology workflow

3. Results and Discussion

As mentioned above, the proposed DBN model consisted of seven input variables, namely depth, breadth, specific gravity, ultimate strength, elasticity modulus, resisting capacity, and induced load. The output of the model was the FRR of timber columns. Given the relatively small size of the dataset, there is an increased risk of overfitting, which can reduce the robustness and generalizability of the DBN model. To address this, the dataset was randomly split into a training set of 48 records (i.e., 80 percent of the entire database) and a testing set of 14 instances (i.e., 20 percent), following standard machine learning practices. The training set was further divided to include a validation subset representing 20% of the training data, enabling monitoring of model performance and early detection of overfitting before evaluating on the testing set.

Additionally, a k-fold cross-validation approach was employed on the training set to further mitigate overfitting and select the best model. In this method, the training data is partitioned into 10 equal folds, with each fold serving as a validation set in turn while the remaining folds are used for training. The model performance evaluation and the comparison between the calculated results with the predicted results from the DBN model are described in detail in the subsequent sections.

3.1. Assessment Categories

The DBN model's performance was evaluated using the coefficient of determination and Root Mean Squared Error, as given in Equations 20 and 21, respectively.

$$R^{2} = 1 - \frac{\sum_{i=1}^{n} (x - \hat{x}_{i})^{2}}{\sum_{i=1}^{n} (x_{i} - \bar{x})^{2}}$$
 (20)

$$RMSE = \sqrt{\frac{1}{n} \sum_{i=1}^{n} (x_i - \hat{x}_i)^2}$$
 (21)

where x_i is the i^{th} actual output; \bar{x} is the mean of the actual outputs; \hat{x}_i is the i^{th} predicted output, and n is the total number of data points.

3.2. Deep Belief Network to Estimate Fire Resistance Rating

The predictive performance of the proposed DBN model was assessed using two coefficients, R^2 and RMSE. Note that the higher value of R^2 and the lower values of RMSE indicate a better prediction capacity of the proposed models. The results of the proposed DBN model's performance are provided in Table 4. As can be seen, the overall coefficient of determination was 0.8775. These results indicate that the proposed DBN model can produce reliable outputs with a high degree of accuracy. For unseen data, the R^2 value was slightly lower, at 0.8623 for the testing dataset. The predictions for the testing data demonstrate that the DBN model can effectively predict outputs for previously unseen input data.

 Data
 R²
 RMSE
 Sample

 Training set
 0.8720
 0.1301
 48

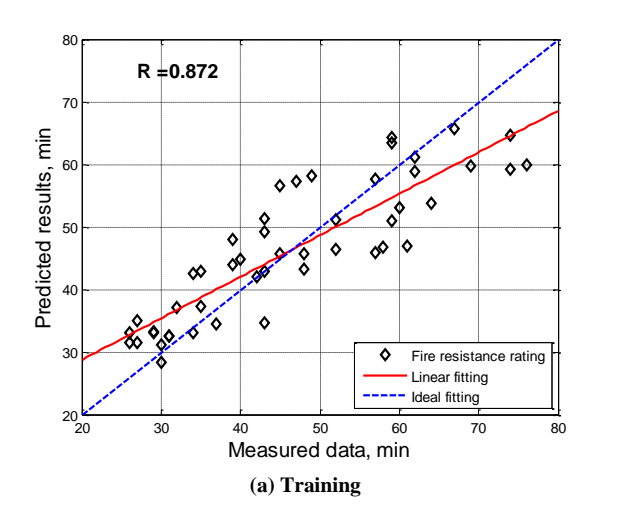
 Testing set
 0.8623
 0.1387
 14

 Overall
 0.8775
 0.1275
 62

Table 3. DBN Model Assessment

Given the present dataset, it is important to note that the proposed DBN model exhibits a strong R^2 value on both training and testing sets, indicating good generalization within the range of parameters represented. However, performance on entirely new experimental conditions outside this range may vary. Future validation with independent or prospective datasets would be necessary to confirm its predictive accuracy under different conditions.

Scatter plots provide an alternative way to visualize the performance of the proposed DBN model. Figure 6 shows the relationship between the timber column FRR predicted by the DBN and the measured values for both training and testing datasets. In the plots, the horizontal axis represents the experimental measurements, while the vertical axis shows the FRR predicted by the model. The black diamond markers represent the experimental data points, while the red solid line indicates the linear fitting of the results, and the blue dashed line corresponds to the ideal 1:1 fitting line. As shown, most of the data points are distributed close to the ideal line, demonstrating good agreement between predicted and experimental values. The linear fitting line also follows the overall trend of the data with a correlation coefficient of $R^2 = 0.872$ and $R^2 = 0.863$ for the training and testing datasets, respectively, indicating a strong positive relationship and confirming the reliability of the predictive model in estimating fire resistance ratings.



5

36

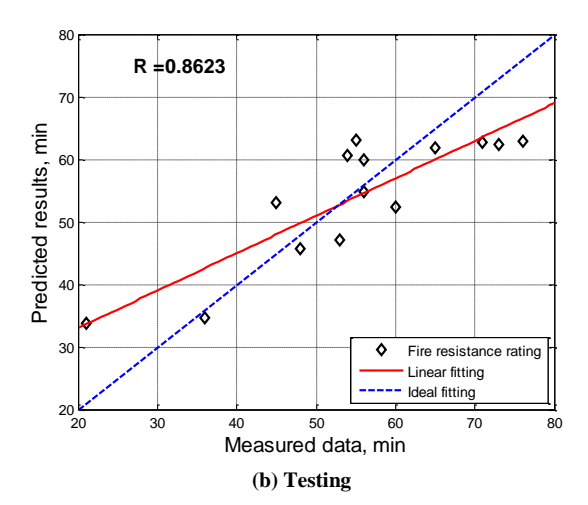


Figure 6. Timber FRR: Predicted vs. Observed Values

3.3. Compared Predicted Results with the Previously Published Calculations

The predicted FRR of timber columns for the testing dataset was compared to the calculated ratings using the empirical equation. Table 5 presents the comparison results. The order of the records in the database is presented in column 1. Columns 2 to 4 contain the experimental ratings, calculated ratings using a mechanics-based method, and predicted ratings from the DBN model, respectively. The predicted rating was rounded to the nearest integer. The difference in percentage between calculated and measured ratings is shown in column 5, and predicted and measured results are presented in column 6. Besides, the information in column 7 represents the instances that the predicted results were better than the calculated values tabulated in the NDS report.

ID Measured (min.) Calculated (min.) Predicted (min.) Cal. and Mea. Diff. (%) Pre. and Mea. Diff (%) **DBN** better **(1) (2)** (3) **(4)** (5) **(6) (7)** $\sqrt{}$ 63 51 55 77 40 14.5 4 21 24 34 14.3 61.9 44 54 64 61 18.5 12.9 54 73 96 62 31.5 15.1 47 32.1 15 53 36 11.3 37 41 62 36.9 4.62 65 35 60 59 52 1.67 13.3 47 60 60 7.14 7.14 56 40 56 55 55 1.79 1.79 14.5 45 76 65 63 17.1 50 53 11.1 17.6 58 45 48 71 63 8.45 11.3 65 1 48 45 46 6.25 4.17

Table 4. Comparison results from the measured and calculated results

As can be seen from Table 4, the proposed DBN model could predict the FRR of the timber columns better than the results from the method using empirical equations proposed in the American Wood Council technical report [1]. To be specific, within the 14 records from the testing dataset, the prediction results from the DBN model showed an equal to or better than that of the results from a mechanics-based method in eight instances. It should be noted that the total number of samples for which the DBN model has shown a better performance was 41 out of 62 records in the entire database.

0.00

2.78

35

36

The SR indicator was used to evaluate the DBN model's computational efficiency [42], representing the percentage of data with relative errors within a specified threshold, as calculated in Equation 22.

$$err_i = \left| \frac{x_i - \hat{x}_i}{x_i} \right| \times 100\%$$
; $SR = \frac{N_{ep}}{N} \times 100\%$ (22)

Where, err_i denotes the relative error; x_i the actual output; \hat{x}_i is the predicted outputs; N_{ep} is the number of data records with a relative error smaller than the restrained error bound, N_{ep} is the number of data points with relative error below the specified threshold, and N is the total number of data points. Figure 7-a illustrates the SR for the full dataset across different methods, while Figure 7-b compares experimental FRR values with predictions from these methods.

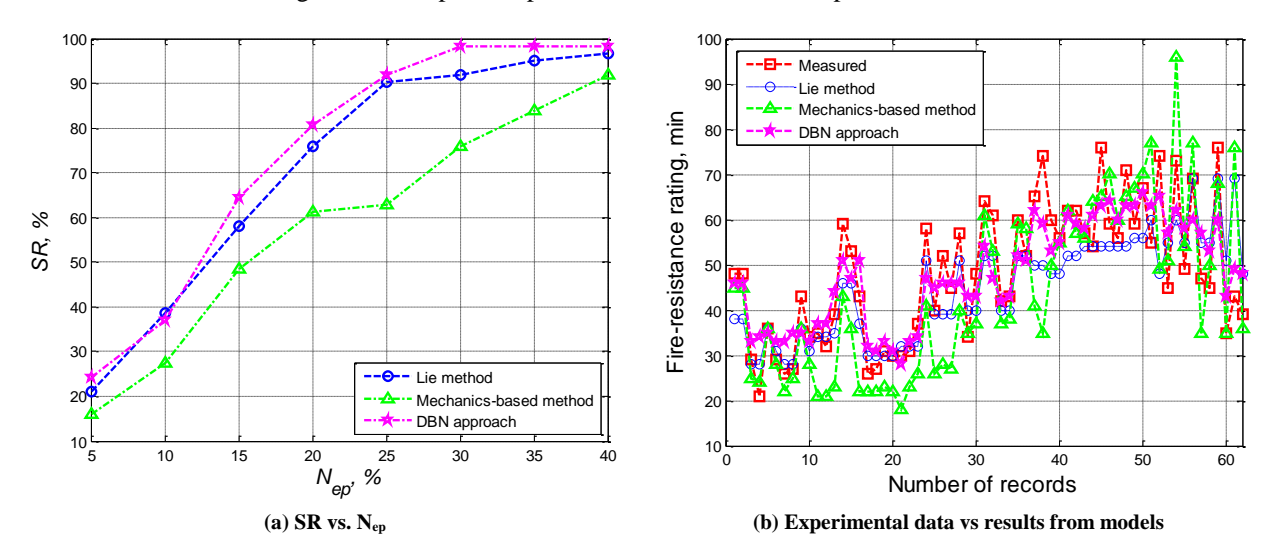


Figure 7. Performance assessment of different models

Figure 7-a compares the predicted FRR of timber columns obtained from the Lie method, the mechanics-based method, and the DBN approach. Among them, the mechanics-based method consistently yields the lowest estimates, demonstrating its conservative nature and tendency to underestimate fire resistance. The Lie method provides intermediate predictions, aligning more closely with the DBN approach at higher values but still showing some deviation. In contrast, the DBN approach consistently predicts higher FRR values, particularly at low and medium ranges, illustrating its capability to capture nonlinear relationships and deliver more accurate predictions. These results suggest that the DBN method offers improved predictive accuracy and less conservativeness compared to conventional approaches.

The comparison by including the measured FRR values alongside the three prediction methods is shown in Figure 7-b. The experimental results show significant variability, reflecting the inherent scatter in fire testing. The Lie method generally underestimates higher values and fails to capture local fluctuations. The mechanics-based method performs less reliably, producing unstable predictions with large deviations from measured values, especially in the mid-to-high ranges. By contrast, the DBN approach demonstrates strong agreement with the measured data, effectively capturing both the overall trend and local variations. This close alignment indicates the robustness and superior predictive capability of the DBN model, confirming its advantage over traditional mechanics-based and semi-empirical approaches in modeling fire resistance of timber columns.

It can be observed that the proposed DBN method presented great predicted results within the range of experimental records. Regarding the calculated results using empirical equations, the equation proposed in the mechanics-based method tended to conservatively predict the FRR for column members. The results using the mechanics-based method showed a high level of inaccuracy in some records. With respect to the calculated results using the Lie method, the calculation underestimated the ratings in most cases. However, the results from the Lie method were less conservative in comparison with those of using the mechanics-based method.

3.4. Inputs and Outputs Relationship

Sensitivity analysis was conducted to examine the effects of input variables on the output. For this purpose, seven DBN models with different combinations of input parameters were developed. The original model DBN0 consisted of all seven input variables. To develop a new model, one variable was taken out of the input parameters of the original model. Specifically, the DBN1 model was created by removing the DEP variable from the input variable of the DBN0 model. Similarly, the DBN2, DBN3, DBN4, DBN5, DBN6, and DBN7 model was developed by eliminating BRH, SPG, ULS, ELM, RCP, and IDL variables from the input of the original DBN0 model, respectively.

In order to achieve a reliable result, each developed DBN model conducted an output estimation ten times. For each trial, 80 percent of the entire database (i.e., 48 records) was arbitrarily chosen to create the training dataset. The value of *RMSE* for the training dataset in each run was recorded. The performance of the developed DBN models was evaluated using the average RMSE over ten trials. The detailed input parameters, performance results, and efficacy ranking of all seven developed DBN models are shown in Table 6.

Table 5. Developed model information and its performance

Name	Input variable	Exclusion var.	RMSE	Ranking
DBN0	DEP, BRH, SPG, ULS, ELM, RCP, IDL	-	0.1286	-
DBN1	BRH, SPG, ULS, ELM, RCP, IDL	DEP	0.1429	5
DBN2	DEP, SPG, ULS, ELM, RCP, IDL	BRH	0.1558	7
DBN3	DEP, BRH, ULS, ELM, RCP, IDL	SPG	0.1372	3
DBN4	DEP, BRH, SPG, ELM, RCP, IDL	ULS	0.1279	2
DBN5	DEP, BRH, SPG, ULS, RCP, IDL	ELM	0.1277	1
DBN6	DEP, BRH, SPG, ULS, ELM, IDL	RCP	0.1410	4
DBN7	DEP, BRH, SPG, ULS, ELM, RCP	IDL	0.1458	6

As can be seen, the DBN4 and DBN5 models presented the best performance results among all seven developed DBN models, with the value of *RMSE* being 0.1279 and 0.1277, respectively. That means the ELM and ULS variables had only a minor influence on the DBN model's predictive capacity. On the other hand, by taking the BRH and IDL variables out of the original input to create the DBN2 and DBN7 models. The developed model showed the least prediction ability, with the value of *RMSE* increased to 0.1558 and 0.1458, respectively. In other words, the BRH and IDL variables had the greatest impact on the predictive accuracy of the DBN model. This finding is consistent with the understanding that increased column breadth enhances thermal mass, slowing heat penetration, while higher applied loads accelerate failure due to the reduction of material strength at elevated temperatures.

4. Conclusion

In this study, a DBN model was developed to predict the FRR of timber columns, using experimental data collected from previously published research. Seven input variables, including depth, breadth, specific gravity, ultimate strength, elastic modulus, resisting capacity, and induced load, were employed to train and optimize the DBN model. The primary objective was to evaluate whether a machine learning-based approach could provide more accurate predictions than conventional empirical methods. To achieve this, the FRR predicted by the DBN model was compared with ratings calculated using established empirical equations, particularly those proposed in the American Wood Council report. The comparison indicated that the DBN model consistently produced predictions closer to the experimental observations, demonstrating its superiority over the traditional calculation methods. This improvement highlights the potential of integrating advanced data-driven models in structural engineering applications, where complex interactions between multiple material and loading parameters often limit the accuracy of empirical formulas.

The performance of the developed DBN model was evaluated using the coefficient of determination, R^2 , yielding values of 0.8623 for the testing dataset and 0.8775 for the overall dataset, reflecting strong predictive accuracy. A sensitivity analysis was conducted to assess the relative importance of each input variable on the model's performance. Results revealed that BRH and IDL were the most influential parameters, suggesting that these variables play a critical role in determining the fire-resistance capacity of timber columns. Conversely, ELM and ULS were found to have the least impact on the model's predictive ability. These findings provide insight into which factors most significantly affect fire-resistance performance and can guide both experimental design and structural assessment. Overall, the study demonstrates that machine learning-based models, such as the DBN, offer a reliable and efficient alternative for predicting the FRR of timber structures, potentially enhancing design safety and optimizing material usage. The adoption of such data-driven approaches represents a promising direction for future research and practical applications in structural fire engineering.

5. Declarations

5.1. Author Contributions

Conceptualization, T.N., H.P., and H.N.; methodology, T.N. and H.P.; software, T.N. and H.N.; investigation, T.N.; resources, T.N., H.P., and H.N.; data curation, H.N. and H.P.; writing—original draft preparation, T.N.; writing—review and editing, H.N. and H.P.; supervision, T.N.; project administration, H.N. and H.P.; funding acquisition, H.N. and H.P. All authors have read and approved the final version of the manuscript.

5.2. Data Availability Statement

The data supporting this study are available from the corresponding author upon request.

5.3. Funding

The authors received no financial support for the research, authorship, and/or publication of this article.

5.4. Conflicts of Interest

The authors declare no conflict of interest.

6. References

[1] Technical Report No. 10. (2018). Calculating the fire resistance of exposed wood members. American Wood Council, Leesburg, United States.

- [2] AWC. (2025). ReThink Wood. Mass Timber in North America. American Wood Council (AWC), Virginia, United States. Available online: https://www.awc.org (accessed on September 2025).
- [3] O'Neill, B. (2019). Architectural Digest. The world's tallest timber-framed building finally opens its doors. Architectural Digest, New York, United States. Available online: https://www.architecturaldigest.com/story/worlds-tallest-timber-framed-building-finally-opens-doors (accessed on September 2025).
- [4] Sumitomo Forestry Group. (2018). New development concept W350 plan for wooden high-rise building. press release. Sumitomo Forestry Group, Tokyo, Japan.
- [5] Stoner, M., & Pang, W. (2020). Simulated Performance of Cross-Laminated Timber Residential Structures Subject to Tornadoes. Frontiers in Built Environment, 6, 88. doi:10.3389/fbuil.2020.00088.
- [6] Nguyen, T. T., Dao, T. N., Aaleti, S., van de Lindt, J. W., & Fridley, K. J. (2018). Seismic assessment of a three-story wood building with an integrated CLT-lightframe system using RTHS. Engineering Structures, 167, 695–704. doi:10.1016/j.engstruct.2018.01.025.
- [7] Bartlett, A. I., Hadden, R. M., & Bisby, L. A. (2019). A Review of Factors Affecting the Burning Behaviour of Wood for Application to Tall Timber Construction. Fire Technology, 55(1), 1–49. doi:10.1007/s10694-018-0787-y.
- [8] Anandan, Y. K., van de Lindt, J. W., Amini, M. O., Dao, T. N., & Aaleti, S. (2021). Experimental Dynamic Testing of Full-Scale Light-Frame-CLT Wood Shear Wall System. Journal of Architectural Engineering, 27(1), 4020042. doi:10.1061/(asce)ae.1943-5568.0000443.
- [9] Bader, T.K., Ormarsson, S. (2023). Modeling the Mechanical Behavior of Wood Materials and Timber Structures. Springer Handbook of Wood Science and Technology. Springer Handbooks. Springer, Cham, Switzerland. doi:10.1007/978-3-030-81315-4_10.
- [10] Nguyen, T. T., Dao, T. N., Aaleti, S., Hossain, K., & Fridley, K. J. (2019). Numerical Model for Creep Behavior of Axially Loaded CLT Panels. Journal of Structural Engineering, 145(1), 04018224. doi:10.1061/(asce)st.1943-541x.0002219.
- [11] Girompaire, L., & Dagenais, C. (2024). Fire Dynamics of Mass Timber Compartments with Exposed Surfaces: Development of an Analytical Model. Fire Technology, 60(3), 1477–1501. doi:10.1007/s10694-023-01528-y.
- [12] Wiesner, F., Bartlett, A., Mohaine, S., Robert, F., McNamee, R., Mindeguia, J. C., & Bisby, L. (2021). Structural Capacity of One-Way Spanning Large-Scale Cross-Laminated Timber Slabs in Standard and Natural Fires. Fire Technology, 57(1), 291–311. doi:10.1007/s10694-020-01003-y.
- [13] Chu, W., Fang, J., Yang, Y., Tao, S., Shah, H. R., Wang, M., & Wang, Y. (2025). Reaction to Fire of the Timber Structure Encapsulated by Multilayer Mortar Coating Under Uniform Thermal Loading. Fire Technology, 61(1), 183–212. doi:10.1007/s10694-024-01622-9.
- [14] Malaska, M., Alanen, M., Salminen, M., Jokinen, T., & Ranua, R. (2024). Fire Performance of Steel-Timber Hybrid Beam Section. Fire Technology, 60(4), 2581–2600. doi:10.1007/s10694-023-01471-y.
- [15] Wiesner, F., & Bisby, L. (2019). The structural capacity of laminated timber compression elements in fire: A meta-analysis. Fire Safety Journal, 107, 114–125. doi:10.1016/j.firesaf.2018.04.009.
- [16] Crielaard, R., van de Kuilen, J.-W., Terwel, K., Ravenshorst, G., & Steenbakkers, P. (2019). Self-extinguishment of cross-laminated timber. Fire Safety Journal, 105, 244–260. doi:10.1016/j.firesaf.2019.01.008.
- [17] Aryadi, A., Parung, H., Irmawaty, R., & Amiruddin, A. A. (2024). Investigation of the Mechanical Behavior of Full-Scale Experimental Bugis-Makassar Timber House Structures. Civil Engineering Journal, 10(6), 1765–1787. doi:10.28991/CEJ-2024-010-06-04.
- [18] Muszyński, L., Gupta, R., Hong, S. hyun, Osborn, N., & Pickett, B. (2019). Fire resistance of unprotected cross-laminated timber (CLT) floor assemblies produced in the USA. Fire Safety Journal, 107, 126–136. doi:10.1016/j.firesaf.2018.12.008.
- [19] Richter, F., Kotsovinos, P., Rackauskaite, E., & Rein, G. (2021). Thermal Response of Timber Slabs Exposed to Travelling Fires and Traditional Design Fires. Fire Technology, 57(1), 393–414. doi:10.1007/s10694-020-01000-1.
- [20] ASTM E119-20. (2022). Standard Test Methods for Fire Tests of Building Construction and Materials. ASTM International, Pennsylvania, United States. doi:10.1520/E0119-20.
- [21] ICC. (2015). "International Building Code. International Code Council, Washington, D.C., United States.

[22] ANSI/AF&PA NDS-23005. (2005). National design specification (NDS) for wood construction. American National Standards Institute (ANSI), Washington, United States.

- [23] Lie, T. T. (1977). Method for Assessing the Fire Resistance of Laminated Timber Beams and Columns. Canadian Journal of Civil Engineering, 4(2), 161–169. doi:10.1139/177-021.
- [24] Gagnon, S., & Pirvu, C. (2011). CLT Handbook: Cross-Laminated Timber. Report Special Publication 52, FPInnovations, Pointe-Claire, Canada.
- [25] Tasdemir, S., Altin, M., Pehlivan, G. F., Saritas, I., Erkis, S. D. B., & Tasdemir, S. (2015). Determining fire resistance of wooden construction elements through experimental studies and artificial neural network. Engineering and Technology, International Journal of Chemical, Molecular, Nuclear, Materials and Metallurgical Engineering, 9(1), 209-213.
- [26] Cachim, P. B. (2011). Using artificial neural networks for calculation of temperatures in timber under fire loading. Construction and Building Materials, 25(11), 4175–4180. doi:10.1016/j.conbuildmat.2011.04.054.
- [27] Naser, M. Z. (2019). Fire resistance evaluation through artificial intelligence A case for timber structures. Fire Safety Journal, 105, 1–18. doi:10.1016/j.firesaf.2019.02.002.
- [28] Zaker Esteghamati, M., Gernay, T., & Banerji, S. (2023). Evaluating fire resistance of timber columns using explainable machine learning models. Engineering Structures, 296, 116910. doi:10.1016/j.engstruct.2023.116910.
- [29] Luo, J., Tian, G., Xu, C., Zhang, S., & Liu, Z. (2025). Temperature Field Prediction of Glulam Timber Connections Under Fire Hazard: A DeepONet-Based Approach. Fire, 8(7), 280. doi:10.3390/fire8070280.
- [30] Ye, Z., Hsu, S.-C., & Wei, H.-H. (2022). Real-time prediction of structural fire responses: A finite element-based machine-learning approach. Automation in Construction, 136, 104165. doi:10.1016/j.autcon.2022.104165.
- [31] Ishtiaq, N., W. Loh, T., & T.Q. Nguyen, K. (2024). Using Machine Learning to Improve Fire Safety of Timber Structures. Wood Industry Impacts and Benefits, IntechOpen, London Kingdom. doi:10.5772/intechopen.1006895.
- [32] Amin, R., Mo, Y., Richter, F., Kurzer, C., Werther, N., & Rein, G. (2024). Correction: Predicting the Average Charring Rate of Mass Timber Using Data-Driven Methods for Structural Calculations. Fire Technology, 61(2), 1023–1024. doi:10.1007/s10694-024-01632-7.
- [33] Han, T., Zhang, Z., & Wu, W. (2025). Fire resistance rating prediction of timber-to-steel connections and design optimization informed by explainable machine learning. Engineering Applications of Artificial Intelligence, 156, 111127. doi:10.1016/j.engappai.2025.111127.
- [34] Fud, G. (2018). Deep belief network based ensemble approach for cooling load forecasting of air-conditioning system. Energy, 148, 269–282. doi:10.1016/j.energy.2018.01.180.
- [35] Rafiei, M. H., Khushefati, W. H., Demirboga, R., & Adeli, H. (2017). Supervised Deep Restricted Boltzmann Machine for Estimation of Concrete. ACI Materials Journal, 114(2), 237–244. doi:10.14359/51689560.
- [36] Hao, X., Guo, T., Huang, G., Shi, X., Zhao, Y., & Yang, Y. (2020). Energy consumption prediction in cement calcination process: A method of deep belief network with sliding window. Energy, 207, 118256. doi:10.1016/j.energy.2020.118256.
- [37] Nguyen, T. T., Tung, P. T., Tan, N. N., Linh, N. N., & Luc, T. T. (2022). A Study of Factors Affecting GPR Signal Amplitudes in Reinforced Structures Using Deep Belief Networks. Infrastructures, 7(9), 123. doi:10.3390/infrastructures7090123.
- [38] Nguyen, T. T., & Dinh, K. (2019). Prediction of bridge deck condition rating based on artificial neural networks. Journal of Science and Technology in Civil Engineering (STCE) NUCE, 13(3), 15–25. doi:10.31814/stce.nuce2019-13(3)-02.
- [39] Li, L., & Betti, R. (2023). A machine learning-based data augmentation strategy for structural damage classification in civil infrastructure system. Journal of Civil Structural Health Monitoring, 13(6–7), 1265–1285. doi:10.1007/s13349-023-00705-5.
- [40] Lu, P., Guo, S., Zhang, H., Li, Q., Wang, Y., Wang, Y., & Qi, L. (2018). Research on Improved Depth Belief Network-Based Prediction of Cardiovascular Diseases. Journal of Healthcare Engineering, 8954878. doi:10.1155/2018/8954878.
- [41] Nguyen, T. T., & Dinh, K. (2020). An artificial intelligence approach for concrete hardened property estimation. Journal of Science and Technology in Civil Engineering (STCE) NUCE, 14(2), 40–52. doi:10.31814/stce.nuce2020-14(2)-04.
- [42] Nguyen, T. T., Pham Duy, H., Pham Thanh, T., & Vu, H. H. (2020). Compressive Strength Evaluation of Fiber-Reinforced High-Strength Self-Compacting Concrete with Artificial Intelligence. Advances in Civil Engineering, 3012139. doi:10.1155/2020/3012139.
- [43] Tanaka, M. (2013). Deep Neural Network. Available online: https://www.mathworks.com/matlabcentral/fileexchange/42853-deep-neural-network14 (accessed on September 2025).
- [44] Fischer, A., & Igel, C. (2014). Training restricted Boltzmann machines: An introduction. Pattern Recognition, 47(1), 25–39. doi:10.1016/j.patcog.2013.05.025.

[45] Hinton, G. E., Osindero, S., & Teh, Y. W. (2006). A fast learning algorithm for deep belief nets. Neural Computation, 18(7), 1527–1554. doi:10.1162/neco.2006.18.7.1527.

- [46] Xu, F., Fang, Z., Tang, R., Li, X., & Tsui, K. L. (2020). An unsupervised and enhanced deep belief network for bearing performance degradation assessment. Measurement: Journal of the International Measurement Confederation, 162, 107902. doi:10.1016/j.measurement.2020.107902.
- [47] Lv, Z., & Qiao, L. (2020). Deep belief network and linear perceptron based cognitive computing for collaborative robots. Applied Soft Computing Journal, 92, 106300. doi:10.1016/j.asoc.2020.106300.
- [48] Han, I. J., Yuan, T. F., Lee, J. Y., Yoon, Y. S., & Kim, J. H. (2019). Learned prediction of compressive strength of GGBFS concrete using hybrid artificial neural network models. Materials, 12(22), 3708. doi:10.3390/ma12223708.